JVI Journals.ASM.org

Neutralizing Polyclonal IgG Present during Acute Infection Prevents Rapid Disease Onset in Simian-Human Immunodeficiency Virus $SHIV_{SF162P3}$-Infected Infant Rhesus Macaques

J. Pablo Jaworski,[a] James Kobie,[b] Zachary Brower,[a] Delphine C. Malherbe,[a] Gary Landucci,[h] William F. Sutton,[a] Biwei Guo,[a] Jason S. Reed,[a,c] Enrique J. Leon,[a,c] Flora Engelmann,[a,c] Bo Zheng,[b] Al Legasse,[a] Byung Park,[e] Mary Dickerson,[a] Anne D. Lewis,[a] Lois M. A. Colgin,[a] Michael Axthelm,[a,c] Ilhem Messaoudi,[a,c,d] Jonah B. Sacha,[a,c,d] Dennis R. Burton,[f,g] Donald N. Forthal,[h] Ann J. Hessell,[a,c] Nancy L. Haigwood[a,c,d]

Oregon National Primate Research Center, Oregon Health & Science University, Beaverton, Oregon, USA[a]; University of Rochester, Rochester, New York, USA[b]; Vaccine & Gene Therapy Institute, Beaverton, Oregon, USA[c]; Molecular Microbiology & Immunology[d] and Knight Cancer Institute,[e] School of Medicine, Oregon Health & Science University, Portland, Oregon, USA; Immunology and Microbial Science and IAVI Neutralizing Antibody Center, The Scripps Research Institute, La Jolla, California, USA[f]; Ragon Institute of MGH, MIT, and Harvard, Boston, Massachusetts, USA[g]; University of California Irvine, School of Medicine, Irvine, California, USA[h]

Simian-human immunodeficiency virus (SHIV) models for human immunodeficiency virus (HIV) infection have been widely used in passive studies with HIV neutralizing antibodies (NAbs) to test for protection against infection. However, because SHIV-infected adult macaques often rapidly control plasma viremia and any resulting pathogenesis is minor, the model has been unsuitable for studying the impact of antibodies on pathogenesis in infected animals. We found that $SHIV_{SF162P3}$ infection in 1-month-old rhesus macaques not only results in high persistent plasma viremia but also leads to very rapid disease progression within 12 to 16 weeks. In this model, passive transfer of high doses of neutralizing IgG (SHIVIG) prevents infection. Here, we show that at lower doses, SHIVIG reduces both plasma and peripheral blood mononuclear cell (PBMC)-associated viremia and mitigates pathogenesis in infected animals. Moreover, production of endogenous NAbs correlated with lower set-point viremia and 100% survival of infected animals. New SHIV models are needed to investigate whether passively transferred antibodies or antibodies elicited by vaccination that fall short of providing sterilizing immunity impact disease progression or influence immune responses. The 1-month-old rhesus macaque SHIV model of infection provides a new tool to investigate the effects of antibodies on viral replication and clearance, mechanisms of B cell maintenance, and the induction of adaptive immunity in disease progression.

Following human immunodeficiency virus type 1 (HIV-1) infection, neutralizing antibodies (NAbs) can be measured against the infecting or autologous virus within a few weeks to months, and in a subset of individuals, these mature after 3 years or more to neutralize heterologous isolates (1–3). The apparently slow kinetics of antibody development suggest that NAbs are at a disadvantage in contributing to viral control, relegated to chasing the ever-changing Env protein, which is notorious for shielding its conserved receptor binding regions and shifting its conformation to expose variable regions (4). Human neutralizing monoclonal antibodies (NMAbs) with highly potent activity against a broad range of heterologous HIV isolates have been described (5–8), but these are rare antibodies that have been found in only a small percentage of chronically infected individuals. HIV-1 (9) and simian immunodeficiency virus (SIV) (10) have been shown to cause damage to the B cells in the periphery (11) and in the gut (12), further limiting, though not abolishing, the host humoral response to HIV and to other pathogens (13, 14). Thus, one of the goals of vaccination is to establish B-cell memory that can be efficiently recruited upon virus exposure to develop antibodies that are directed at conserved determinants in order to prevent or control infection. By controlling infection, it may be possible to protect the B-cell compartment as well as slow the loss of $CD4^+$ T cells.

Rhesus macaques have been the primary species utilized in antibody protection studies against mucosal challenge with CCR5 using simian-human immunodeficiency viruses (SHIVs). The use of SHIVs bearing the HIV Env protein has been necessitated by the lack of neutralization of SIV by HIV Env-specific antibodies. The goal of these protection studies has been to examine the effectiveness of various doses of human NMAbs in blocking infection as an all-or-none effect. In that setting, passive administration of NAbs or NMAbs before challenge can fully protect against high-dose intravenous or mucosal SHIV challenge (15–18). Smaller amounts of NMAbs can reduce infection susceptibility in repeated low-titer mucosal SHIV challenge in macaques (19). Juvenile macaques treated during acute SIV infection with high-dose neutralizing polyclonal IgG purified from SIV-infected macaques (SIVIG) developed NAbs and polyfunctional $CD4^+$ T cells and controlled viremia (20, 21). However, because infection of juvenile or adult macaques with SHIVs that utilize the chemokine receptor CCR5 typically results in well-controlled postacute viremia (22, 23), it has not been possible to determine the effects of NAbs upon disease progression.

Received 24 March 2013 **Accepted** 8 July 2013
Published ahead of print 24 July 2013
Address correspondence to Nancy L. Haigwood, haigwoon@ohsu.edu.
Supplemental material for this article may be found at http://dx.doi.org/10.1128/JVI.00049-13.

doi:10.1128/JVI.00049-13
The authors have paid a fee to allow immediate free access to this article.

We have developed models of $SHIV_{SF162P3}$ infection in adult (24) and 1-month-old (25) pigtail macaques to examine the role of antibodies in limiting infection. As we reported in a prior publication (24), we observed variable pathogenesis in newborn pigtail macaques infected by exposure from their dams, which were infected with $SHIV_{SF162P3}$ with only one baby infected *in utero* developing rapid disease progression. Direct oral infection of baby pigtails, which was the same route we used with the 1-month-old rhesus infants, resulted in pathogenesis (at week 9) in only 1 of the 4 infected babies despite the loss of CD4 cells in 3 of 4. In adult pigtails infected intravenously, we did not see any signs of disease until week 20, and only 2 of 8 animals were lost due to disease by 30 weeks (only 1/8 with CD4 loss). Moreover, in our 2010 publication on 1-month-old infant pigtails, there was no evidence of pathogenesis in the 6-month period of study despite very high persistent viremia (25). Here, we observed that like 1-month-old pigtail macaques, 1-month-old rhesus macaques infected orally with $SHIV_{SF162P3}$ develop chronic infection with persistently high (10^7 to 10^8 copies/ml) plasma viremia and concomitant development of HIV Env-specific NAbs. However, to our surprise, rhesus macaques were more susceptible to virus-induced disease than pigtails, and many of these very young macaques progressed quickly within 12 weeks of infection. Thus, to investigate the impact of IgG purified from SHIV-infected macaques (SHIVIG) in modulating the host response to severe pathogenesis, we performed passive studies in 1-month-old rhesus macaques. The goal of these studies was to utilize this highly pathogenic virus/host combination to better understand whether the presence of NAbs during acute infection could provide an immunomodulatory effect to normalize the adaptive responses and mitigate the rapid disease onset observed in control animals. Because of the persistent viremia, we also found that it was possible to measure a significant degree of control in rhesus macaques that had certain major histocompatibility complex class I (MHC-I) alleles, allowing us to show a very strong correlation between the presence of certain alleles of MHC-I, *Mamu-B*08* and *Mamu-B*17*, and a lower level of viremia in the set-point stage of the disease previously shown to control SIVmac239 viremia (26, 27). This knowledge is critical for optimal future study design. In short, the 1-month-old rhesus model now enables us to demonstrate for the first time that passive NAb treatment prior to viral exposure could mitigate severe viral pathogenesis, improving the rate and duration of survival while decreasing viremia.

Passive treatment in this study not only led to lower levels of integrated virus but also preserved B cells, resulting in accelerated NAb and antibody-dependent cell-mediated viral inhibition (ADCVI) development and the protection of infected 1 month olds from rapid disease progression. Due to the rapid pathogenesis and uniform viremia, this model offers an option to compare antibodies with differing modes of action for their effectiveness *in vivo*. It would also allow the testing of polyclonal antibodies generated by vaccines for their effectiveness in blocking infection and whether they contribute to facilitating adaptive humoral responses or protection from rapid disease onset.

MATERIALS AND METHODS

Ethics statement. All animal work is regulated by the Office of Laboratory Animal Welfare and the U.S. Department of Agriculture and National Institutes of Health guide for the care of laboratory animals, and the facilities at the Oregon National Primate Research Center are accredited by the American Association for Accreditation of Laboratory Animal Care. There is no alternative to the use of nonhuman primates to study the pathogenesis of viruses related to HIV-1 and how the virus stimulates the immune responses *in vivo*. The experimental protocols were approved by the Oregon Health & Science University Institutional Animal Care and Use Committee. All macaques were pair-housed for this study and provided with enrichment activities and species-appropriate treats. All procedures involving potential pain were performed with the appropriate anesthetic or analgesic. The number of animals used in this study was scientifically justified based on statistical analyses of virological and immunological outcomes.

Macaques. Seven-day-old rhesus macaques (*Macaca mulatta*) were obtained from the breeding colony and raised for 3 weeks in the animal biosafety level 2 (ABSL-2) infant nursery at the Oregon National Primate Research Center in Beaverton, OR (ONPRC). At 1 month of age, after adaptation to formula feeding, animals were transferred to containment for study procedures.

IgG preparations. IgG purification was performed as previously described (20). Normal IgG was purified from 1 liter of pooled plasma from seven simian retrovirus- and SIV-negative adult rhesus macaques screened for the absence of reactivity to HIV-1 SF162 gp140 (by enzyme-linked immunosorbent assay [ELISA]) and the absence of neutralization against $SHIV_{SF162P3}$ (TZM-bl assay). SHIVIG formulations A and B were purified from 200 and 110 ml, respectively, of pooled plasma obtained from terminal bleeds of macaques that were infected with $SHIV_{SF162P3}$ for 6 months. The two SHIVIG formulations showed similar *in vitro* neutralizing properties. IgG1 b12 was combined with SHIVIG at a ratio of 1:1,000 (wt/wt). Normal IgG was combined with the MAb IgG1 b12 at the same ratio as that used in the previous group (1:1,000, wt/wt). Purity of >90% was determined by SDS-PAGE.

Virus challenge and IgG administration. In this study, we used $SHIV_{SF162P3}$ (passage 3) virus, which has been described elsewhere (22, 28). We obtained $SHIV_{SF162P3}$ through the NIH AIDS Research and Reference Reagent Program, Division of AIDS, National Institute of Allergy and Infectious Diseases, NIH (catalog number 6526; contributors J. Harouse, C. Cheng-Mayer, and R. Pal). Twenty-four newborn rhesus macaques were divided into 4 groups, with 6 animals per group. Purified IgG was delivered subcutaneously at multiple sites around the scruff of the neck and the back of the animals 24 h before oral virus challenge with two doses of 50% animal infectious doses (AID_{50}) ($\sim 7 \times 10^8$ viral RNA copies) of a macaque cell-grown stock of $SHIV_{SF162P3}$ administered 15 min apart. AID_{50} was determined in a titration experiment described previously (24). Infants were monitored for 6 months for clinical signs of disease, including lymph node palpation and measurement, weight, appetite, etc. Blood samples were taken at weekly, biweekly, or monthly intervals to determine lymphocyte subsets, antibody responses, and viral load in plasma and in peripheral blood mononuclear cells (PBMC).

Cell-associated viral load. PBMC DNA was extracted using a QiaAmp DNA blood mini kit (Qiagen) according to the manufacturer's instructions. Proviral load was measured by quantitative PCR (qPCR). PCRs for SHIV DNA contained TaqMan universal PCR master mix (ABI, Norwalk, CT), 500 nM forward and reverse primers (GAG5f, 5′-ACTTTCGGTCT TAGCTCCATTAGTG-3′; GAG3r, 5′-TTTTGCTTCCTCAGTGTGTTT CA-3′), and 200 nM TaqMan probe labeled with a 5′ 6-carboxyfluorescein (FAM) fluorescent reporter dye and a 3′ black hole quencher (BHQ) (5′-FAM-TTCTCTTCTGCGTGAATGCACCAGATGA-BHQ 6-carboxy tetramethylrhodamine-3′). Real-time PCR was performed on an ABI 7500 Fast machine (ABI) with the following cycling conditions: 2 min at 50°C, 95°C for 10 min, and then 45 cycles at 95°C for 15 s and at 60°C for 1 min. Standards were dilutions of genomic DNA from Hut-78/E11S cells, which contain one copy of SIV *gag* per genome. Two positive and two negative controls were included in each tested plate.

Plasma viral load. Viral stock RNA and plasma viral RNA samples were extracted using the QIAamp viral RNA extraction kit (Qiagen) per the manufacturer's instructions. The RNA copy number was measured by

quantitative RT-PCR (RT-qPCR). RT reactions consisted of 500 μM deoxynucleoside triphosphates (dNTPs), 2.5 ng μl^{-1} random hexamers, 0.6 U/μl RnaseOut, 5.7 U/μl SuperScript III (Invitrogen) in a total volume of 14 μl. RT reaction conditions included 25°C for 10 min, followed by 42°C for 50 min and then 85°C for 5 min. To quantify cDNA, 2 μl of the RT reaction was used in the quantitative PCR described above in a total volume of 30 μl. The standard for RNA was an *in vitro* transcript of plasmid p239gag containing the KpnI-BamHI SIV *gag* fragment from SIVmac239 (gift of J. Lifson and M. Piatak). Tenfold dilutions of this standard were made from 1×10^6 to 10 copies μl^{-1}. A final 2-fold dilution was made to obtain 5 copies μl^{-1}. High-, intermediate-, and weak-positive controls, as well as negative controls, were included in each plate.

Pseudovirus construction. The cloning of *env* sequences derived from the $SHIV_{SF162P3}$ virus stock has been previously described (25). Individual *env* clones contained within the pEMC* expression plasmid were cotransfected with the *env*-deleted viral backbone plasmid Q23Δ*env* (kindly provided by Julie Overbaugh [29]).

TZM-bl neutralization assay. Plasma samples from each animal were tested at all available time points for neutralizing activity using the 96-well TZM-bl neutralization assay described previously (30).

ELISA. ELISA was used to assess the presence of gp140-specific antibodies as previously described (31).

ADCVI assay. The ADCVI assay was performed as previously described (32).

MHC-I genotyping. Animals were MHC-I genotyped for *Mamu-A*100101* (*A*01*), *Mamu-A*002:01* (*A*02*), *Mamu-A*008:01* (*A*08*), *Mamu-B*001:0101* (*B*01*), *Mamu-B*008:01* (*B*08*), and *Mamu-B*017:01* (*B*17*) by sequence-specific priming PCR (PCR-SSP) amplification using primers and cycling conditions as previously published (33).

MHC-I-restricted $CD8^+$ T cell responses. IFN-γ ELISPOT assay was performed using frozen PBMC from acute or chronic infection as previously described (34). Briefly, 1×10^5 frozen PBMC were incubated in duplicate overnight with 10 μM the indicated minimal optimal peptide or with a Gag open reading frame peptide pool, which contained every 15-mer peptide (overlapping by 11 amino acids) spanning SIVmac239 Gag. Results are shown for spot-forming cells (SFCs) per 1×10^6 PBMC following subtraction of duplicate wells containing media only (negative control). Results are considered positive if the level was greater than twice the background and greater than 50 SFCs/1×10^6 PBMC.

Intracellular cytokine staining. Cells were obtained from bronchoalveolar lavage (BAL) fluid samples at necropsy. Intracellular cytokine staining of IFN-γ and tumor necrosis factor alpha (TNF-α) was performed as previously described (35). Samples were analyzed using the LSRII instrument (BD Biosciences, San Jose, CA) and FlowJo software (TreeStar, Ashland, OR).

Single-genome amplification and Env sequence analysis. cDNA was generated with oligo(dT) using the SuperScript III first-strand synthesis system (Invitrogen, Carlsbad, CA) from plasma viral RNA of two IgG1b12-treated animals (B29003 and B29081) and two normal IgG-treated animals (N28776 and N28778) at 1 week postinfection (p.i.) as well as from the viral inoculum. Single-genome amplification (SGA) of full-length gp160 envelope was performed according to the CHAVI standard operating procedure (36) using high-fidelity platinum *Taq* (Invitrogen, Carlsbad, CA) and primers designed specifically for this study. First-round primers for gp160 SGA amplification were BGenv5out (GCTATA CCGCCCTCTAGAAGC) and BGenv3out (GGCCTCACTGATACCCCT ACC). The first-round conditions were denaturation at 94°C for 2 min; 35 cycles of 94°C for 15 s, 58°C for 30 s, and 68°C for 4 min; and a final elongation at 68°C for 15 min. Second-round primers for gp160 SGA amplification were BGenv5in (GGCAGGAAGAAGCGGAGACAGC) and BGenv3in (GACGGCCTGGACCGCCTCATGG). The second-round conditions were denaturation at 94°C for 2 min; 45 cycles of 94°C for 15 s, 58°C for 30 s, and 68°C for 4 min; and a final elongation at 68°C for 15 min. Upon satisfying the SGA criteria of fewer than 30% positive results, the 2.85-kb PCR products were treated with exoSAP-IT (Affymetrix, Santa Clara, CA) and analyzed by DNA sequencing using BigDye Terminator v3.1 sequencing kits on an Applied Biosystems 3730XL DNA analyzer (Applied Biosystems, Foster City, CA). The sequencing primers were 218 (ATCATTACACTTTAGAATCGC), ED5P3mod (ATGGGATCAAA GTCTAGAGCCATGTG), KK1 (GCACAGTACAATGTACACATGG AA), env8R (CACAATCCTCGCTGCAATCAAG), and env6For (GAAT TGGATAAGTGGGCAAG). Sequences with early stop codons or with double peaks were discarded. Full-length contigs were built with the Sequencher software program (Gene Codes Corporation, Ann Arbor, MI). Duplicate sequences were identified by ElimDupes (http://www.hiv.lanl.gov/content/sequence/ELIMDUPES/elimdupes.html) and were removed from further analysis. Unique full-length nucleotide sequences were aligned to JR-CSF (accession no. U45960) and HxB2 (accession no. K03455) with HIVAlign (http://www.hiv.lanl.gov/content/sequence/VIRALIGN/viralign.html). The protein alignments were manually annotated on Geneious Pro software 5.4.6 (Biomatters, Auckland, New Zealand) according to HxB2 numbering. Previous studies identified amino acid mutations that affect neutralization sensitivity to IgG1 b12 in the context of the JR-CSF envelope (37, 38). We used these data as references to assess whether mutations were present at these amino acid positions in the envelope sequences cloned in the present study.

B-cell ELISPOT assay. Quantitation of gp140-specific memory B cells was performed with methods similar to those described previously (39). Briefly, cryopreserved peripheral blood lymphocytes were thawed and cultured at 2×10^6 cells/ml in 500 μl media (RPMI 1640, 10% fetal calf serum, 1% penicillin-streptomycin, 1% nonessential amino acids, 1% sodium pyruvate, 10 mM HEPES) containing 5 μg/ml CpG 10103 (TLR9 agonist; Oligos Etc., Wilsonville, OR), 2.5 μg/ml R848 (TLR 7/8 agonist; Invivogen, San Diego, CA), 1:10,000 *Staphylococcus aureus* Cowan strain (Calbiochem, Rockland, MA), 1:100,000 pokeweed mitogen (PWM; Sigma-Aldrich, St. Louis, MO), and 100 ng/ml interleukin-2 (IL-2; Peprotech, Rocky Hill, NJ) in 48-well flat-bottom plates for 4 days at 37°C and 5% CO_2. Enzyme-linked immunosorbent spot (ELISPOT) plates (MSIPN4W50; 96-well; Millipore, Bedford, MA) were coated overnight at 4°C with either 3 μg/ml purified oligomeric SF162 gp140 prepared as previously described (40) or 2 μg/ml anti-rhesus IgG (3H12; NHP Reagent Resource, Boston, MA) in phosphate-buffered saline (PBS). Coated plates were blocked with media for 2 h. For gp140 detection, 20,000 to 500,000 cultured PBMC per well were incubated at 37°C for 18 to 20 h. For total IgG determination, 800 to 20,000 cultured PBMC per well were added. After incubation, cells were aspirated and plates were washed with PBS with 0.1% Tween. Bound antibodies were detected with 2 μg/ml biotinylated anti-human IgG (BD Biosciences, San Jose, CA) for 1 h and with 1:1,000 streptavidin-alkaline phosphatase (SouthernBiotech, Birmingham, AL) for 45 min and developed with Vector blue alkaline phosphatase substrate kit III (Vector Laboratories, Burlingame, CA). Spots in each well were counted using the CTL immunospot reader (Cellular Technologies Ltd., Shaker Heights, OH).

Statistics. To analyze the effect of the treatment on viremia control and the elicitation of *de novo* NAbs, the SHIVIG group consisted of six macaques ($n = 6$) and the No-SHIVIG group consisted of eight macaques ($n = 8$). To measure the median change in virus loads and antibody levels ($n = 14$), the area under the curve (AUC; from 0 to 24 weeks postinfection) was calculated. Statistical significance was determined using the Mann-Whitney U test. Contrast *t* tests within repeated-measures analysis of variance (ANOVA) were used to determine statistical significance of mean comparisons at specific time points. To measure the effect of *de novo*-produced NAbs on set-point viremia control and to measure the ability to elicit *de novo* NAbs ($n = 14$), we used the Spearman correlation. The Mann-Whitney U test was also used to determine statistical significance in the comparison of set-point plasma viral loads between *Mamu-B*08-* and *-B*17*-positive and -negative untreated animals ($n = 14$). We used ANOVA to determine statistical significance in the comparisons of the different lymphocyte subsets between NAb^+, NAb^-, and uninfected groups ($n = 19$). The statistical significance in the correlation between

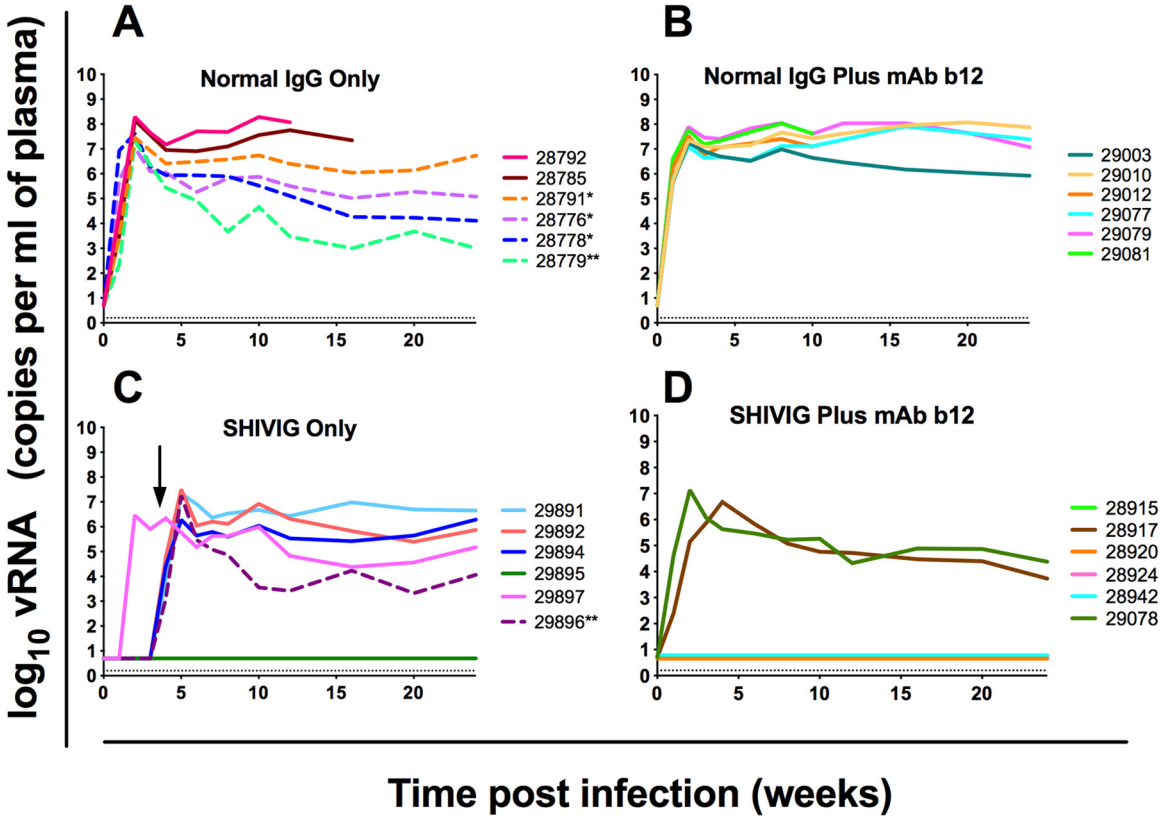

FIG 1 Effect of passively transferred IgG on plasma viral load in $SHIV_{SF162P3}$-infected 1-month-old rhesus macaques. Blood samples were collected at regular intervals after viral exposure, the RNA was isolated from plasma, and viral RNA (vRNA) was quantified by real-time RT-PCR. Curves represent individual infected animals that were treated with normal IgG only ($n = 6$) (A), normal IgG plus MAb b12 ($n = 6$) (B), SHIVIG only ($n = 6$) (C), or SHIVIG plus MAb b12 ($n = 6$) (D) prior to challenge with $SHIV_{SF162P3}$. Animals positive for the *Mamu-B*08* or *-B*17* allele are denoted with dashed lines in the graphs and asterisks in the legends. The dotted line indicates the assay limit of detection. Individual animals are identified.

plasma and cell-associated viral loads ($n = 14$) was assessed by the Spearman test. For differences in binary outcomes, we used Fisher's exact tests to determine statistical significance. Kaplan-Meier survival analysis and the log-rank test ($n = 14$) were used to test for differences in the time to AIDS development, comparing NAb^+ and NAb^- animals. The significance level was set at $P < 0.05$ and is stated in each case.

Nucleotide sequence accession numbers. The unique full-length nucleotide sequences determined in this work were deposited in GenBank under accession numbers JQ672556 to JQ672584.

RESULTS

SHIV postacute plasma viremia in newborn rhesus macaques is impacted by MHC-I alleles. To determine the characteristics of $SHIV_{SF162P3}$ in newborn rhesus macaques, we exposed six macaques to the virus by oral inoculation as previously performed in newborn pigtails (24, 25). In preparation for passive transfer studies with antibodies, we exposed newborn rhesus macaques after infusion of normal IgG at 200 mg/kg of body weight. Purified IgG was administered subcutaneously, followed by oral inoculation 24 h later with 10 AID_{50} $SHIV_{SF162P3}$. At the same time we tested a group of six macaques, termed normal IgG plus b12, that were infused with normal IgG mixed with NMAb b12 at 0.2 mg/kg, the dose we had previously tested in pigtail macaques in combination with polyclonal SHIVIG. This group was included so that we could formally determine the effects of b12 alone. The dose of b12 at 0.2 mg/kg used in the present study is 125 times less than the fully protective b12 dose given to adult female rhesus macaques in a single high-dose $SHIV_{SF162P4}$ vaginal challenge model (41) and five times less than the b12 dose administered in a low-dose repeated challenge study with $SHIV_{SF162P3}$ (19).

All macaques in the normal IgG-only and normal IgG-plus-b12 groups had detectable plasma viremia at 1 week and similar peak viremia levels 2 weeks after challenge (Fig. 1A and B). In contrast to our previous experience with newborn pigtail macaques infected with $SHIV_{SF162P3}$, set-point plasma viremia in the normal IgG-only group was highly variable and ranged from 1.0×10^3 to 1.5×10^8 copies/ml (25) (Fig. 1A). However, viremia in animals from the normal IgG-plus-b12 group was in a very limited range from 5×10^6 to 1.5×10^8 copies/ml (Fig. 1B). The high variability of viremia in the normal IgG-only group prompted us to test all animals for the presence of MHC-I alleles associated with control of SIVmac239 infection in adult rhesus macaques (26, 27). Groups of newborns were not balanced for these alleles at the outset of the experiment, because there was only limited evidence that one MHC-I allele (*Mamu-A*100101*) (*A*01*) impacts SHIV infection (42). After MHC genotyping, we found that the four macaques with the lowest plasma viremia in the normal IgG-only group carried either the *Mamu-B*008:01* (*B*08*) or *Mamu-B*017:01* (*B*17*) allele (Fig. 1A; also see Table S1 in the supplemental material). Neither of these alleles was present in any of the six animals in the normal IgG-plus-b12 group with high and per-

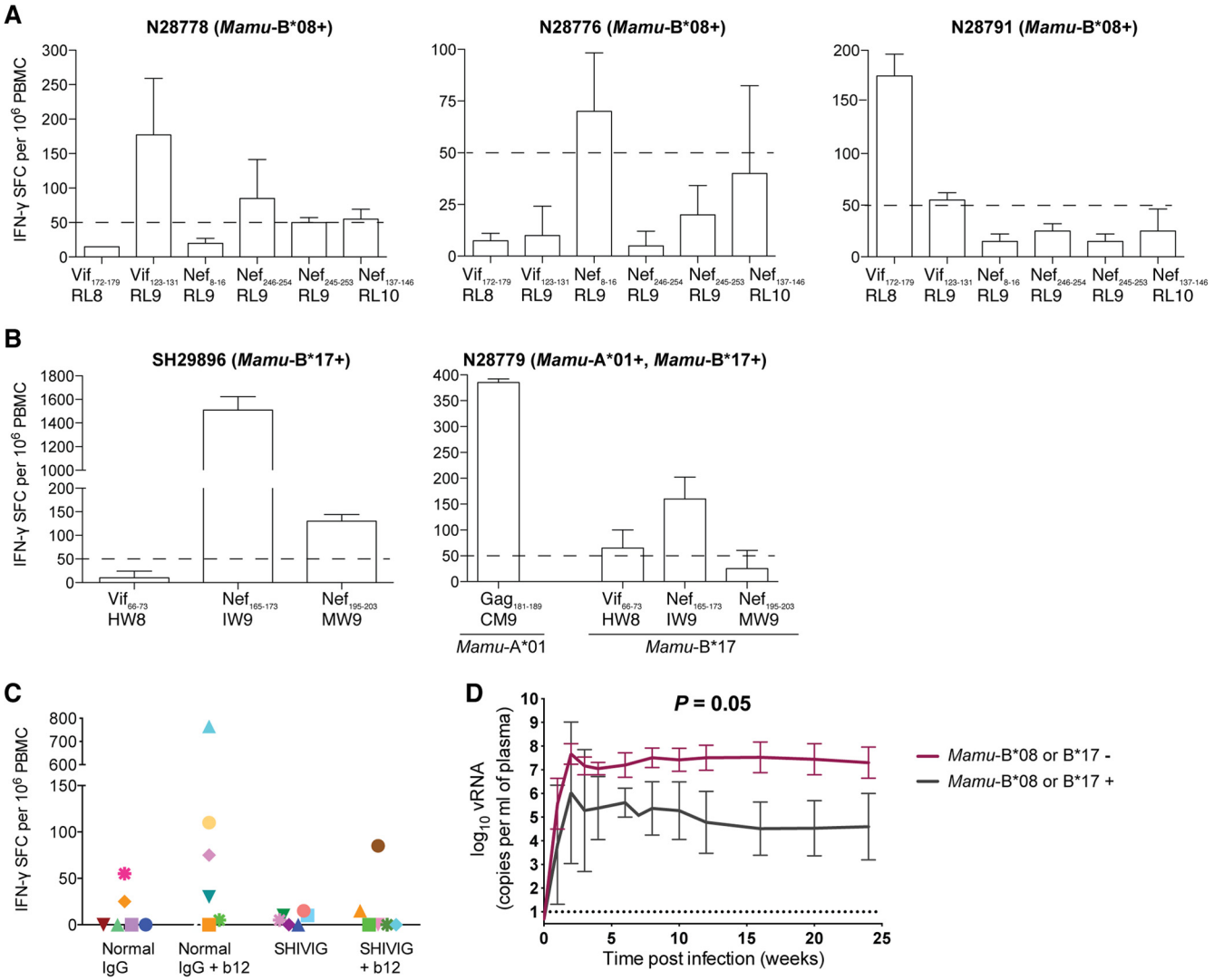

FIG 2 MHC-I-restricted CD8$^+$ T cell responses. To measure MHC-I-restricted CD8$^+$ T cell responses, we performed an IFN-γ ELISPOT assay using frozen PBMC from chronic infection of five macaques infected with $SHIV_{SF162P3}$ and positive for *Mamu-B*08* (A) or for *Mamu-B*17* and for *Mamu-A*01* and *Mamu-B*17* (B). Shown are SFCs per million PBMC for the SIV epitopes indicated following subtraction of duplicate wells containing media (negative control). The dashed line indicates twice the background level. (C) SFCs per million PBMC for each macaque in the study with a Gag open reading frame peptide pool, which contained every 15-mer peptide spanning SIVmac239 Gag. (D) Plasma viral loads as a function of week of infection for *Mamu-B*08*/*B*17*-negative (red line) or *Mamu-B*08*/*B*17*-positive (black line) macaques. $P = 0.05$.

sistent plasma viremia (Fig. 1B). Viremia was significantly lower in *Mamu-B*08*- and *Mamu-B*17*-positive animals than in animals not expressing these MHC-I molecules ($P = 0.05$) (Fig. 2D). $SHIV_{SF162P3}$ lacks the *Mamu-B*08*- and *Mamu-B*17*-bound CD8$^+$ T cell epitopes associated with SIV_{mac239} Env. However, *Mamu-B*08*- and *Mamu-B*17*-restricted CD8$^+$ T cells predominantly target the Vif and Nef proteins, and these SIV_{mac239} proteins are present in $SHIV_{SF162P3}$. Therefore, we screened peripheral blood mononuclear cells for these previously defined CD8$^+$ T cell epitopes. Indeed, *Mamu-B*08*-positive (Fig. 2A) and -*B*17*-positive (Fig. 2B) animals mounted Vif- and Nef-specific CD8$^+$ T cell responses restricted by these two MHC-I molecules. Therefore, we conclude that *Mamu-B*08* and *Mamu-B*17* contributed significantly to the containment of $SHIV_{SF162P3}$, despite this virus lacking key CD8$^+$ T cell epitopes derived from SIV_{mac239} Env. Interestingly, however, the overall SHIV-specific CD8$^+$ T cell response, as measured by the total Gag-specific CD8$^+$ T cell response, was similar between the different experimental groups (Fig. 2C). Thus, while *Mamu-B*08* and -*B*17*-restricted CD8$^+$ T cells likely contributed to set point viral loads in animals expressing these alleles, differences in the overall CD8$^+$ T cell response does not explain the differences in viral load between the groups.

To determine whether the small amount of b12 tested in combination with normal IgG exerted selection pressure on the virus, leading to escape variants (37, 38), we examined the sequences of 25 Env clones from two normal IgG-only and two normal IgG-plus-b12 macaques (36) (see Table S2 in the supplemental material). No evidence of early b12 escape variants was detected.

Due to the unexpected outcome in four out of six animals in the normal IgG group having *Mamu-B*08*/*Mamu-B*17* alleles, we elected to combine the *Mamu-B*08*- and *Mamu-B*17*-negative animals from the normal IgG and the normal IgG-plus-b12

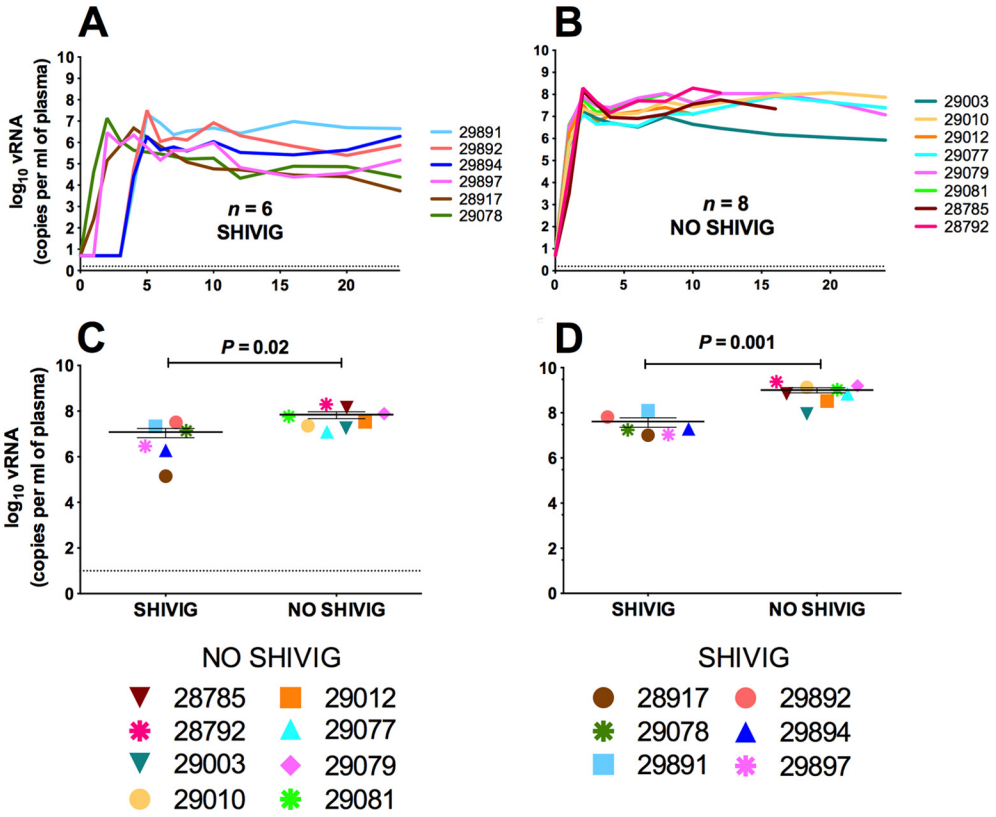

FIG 3 SHIVIG treatment reduces acute and set-point plasma viral load (PVL) in $SHIV_{SF162P3}$-infected infant rhesus macaques. PVL for individual treated animals are compared over the period of the study for SHIVIG ($n = 6$) (A) and No-SHIVIG ($n = 8$) (B). Comparisons of PVL between SHIVIG and No-SHIVIG animals are shown at 2 weeks after challenge (C), and the area under the curve (AUC) for the 24-week study period is shown (D). Individual animals are indicated with unique symbols. *P* values are indicated (Mann-Whitney U test).

groups to make a control group that would allow us to test the effects of SHIVIG treatment. Three out of six animals in the normal IgG-plus-b12 group produced endogenous NAbs. We were not able to discriminate if these responses were individual spontaneous responses or were due to a residual effect of b12, but the beneficial effect of SHIVIG treatment could be measured.

The impact of NAbs present during infection modeled in newborn macaques. Each SHIVIG preparation was assessed *in*

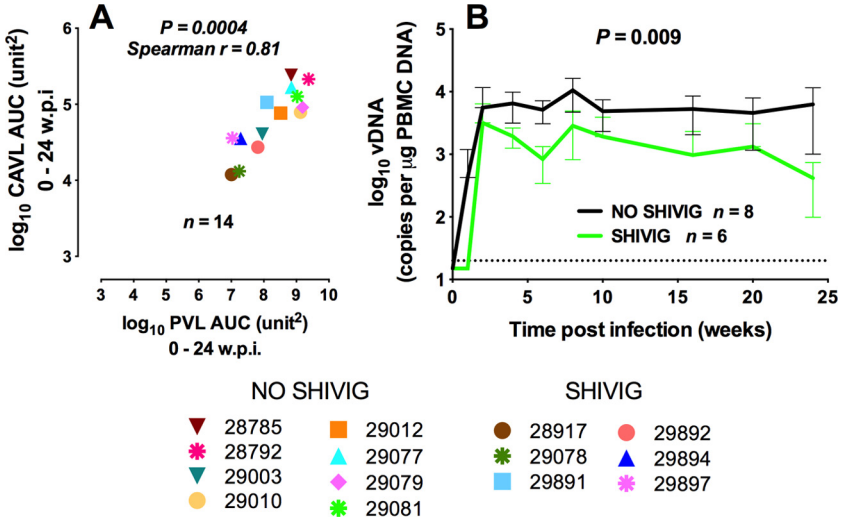

FIG 4 Effect of passively transferred SHIVIG on cell-associated virus load (CAVL). Copies of viral DNA per μg of PBMC cellular DNA were quantified by real-time PCR, and AUC values for weeks 0 to 24 were quantified for individual macaques. (A) Correlation between CAVL and PVL (vRNA per ml of plasma), *P* value, and Spearman rank coefficient (*r*) value are noted. (B) Mean CAVL in SHIVIG versus No-SHIVIG macaques during the 24 weeks after initiation of infection (w.p.i.). The horizontal dotted line shows the limit of detection of the assay. The *P* value is indicated (Mann-Whitney U test).

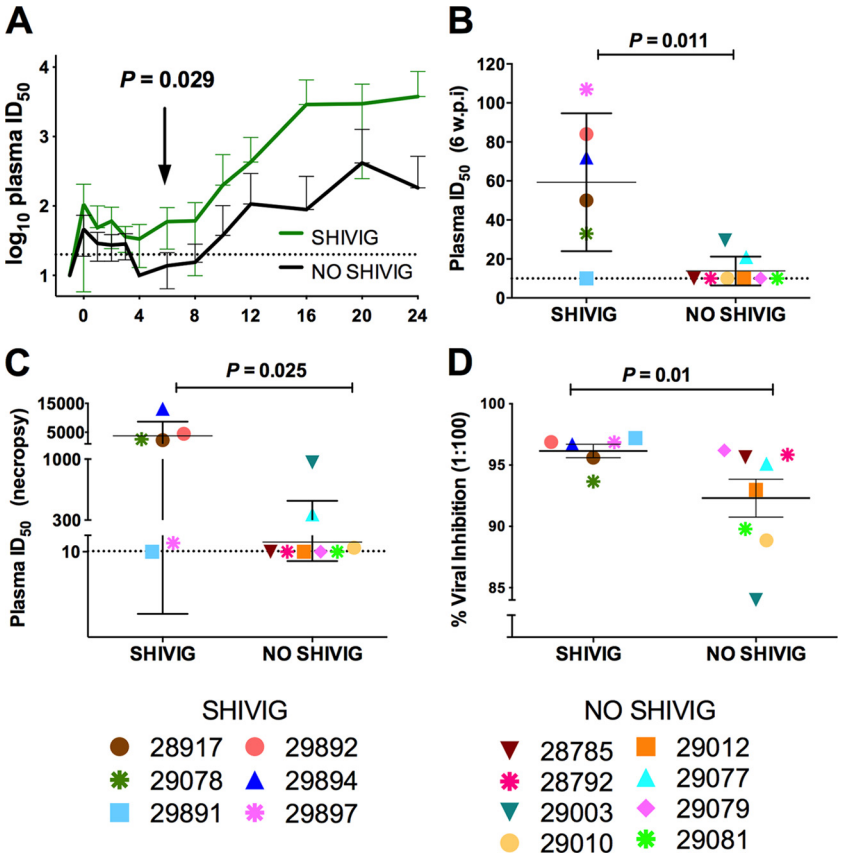

FIG 5 Comparison of neutralizing antibody responses in SHIVIG and No-SHIVIG macaques. (A) Mean NAb titers for the entire 24-week period for SHIVIG and No-SHIVIG animals against $SHIV_{SF162P3}$ clone MC-3, assayed by the TZM-bl neutralization assay. Only the infected and *Mamu-B*08*- and *Mamu-B*17*-negative animals were considered in these analyses ($n = 14$). ID_{50} is the reciprocal of the plasma dilution necessary to inhibit infection by 50%. The horizontal dotted line shows the limit of detection of the assay. The arrow indicates the time for the initiation of the endogenous NAb response. The *P* value is indicated (Mann-Whitney U test). Data shown for individual animals are ID_{50} values at week 6 (B), ID_{50} values at necropsy (C), and plasma ADCVI activity as percent viral inhibition at week 6 (D).

vitro for neutralizing activity against the challenge virus stock ($SHIV_{SF162P3}$), and three molecular clones derived from it, to determine treatment doses that would provide a systemic delivery of neutralizing antibody short of blocking infection (see Table S3 in the supplemental material). In order to evaluate the neutralization sensitivity of the challenge virus, we assessed several pseudotyped $SHIV_{SF162P3}$ envelopes previously cloned (24) from the virus swarm in order to gain a better understanding of the diversity of the neutralization resistance to neutralizing MAbs and to the SHIVIG preparations that would be used in the study. We decided to use the most sensitive clone in order to increase the sensitivity of the TZM-bl assay. This allowed a greater dynamic range for the experiment, including the detection of plasma samples with different degrees of neutralization activity (especially those with lower activity), thereby facilitating comparison among different animals in the various groups. All of the reported neutralization data in the study were generated using the MC-3 $SHIV_{SF162P3}$ cloned envelope in the TZM-bl assay.

We next tested the effects of polyclonal IgG purified from $SHIV_{SF162P3}$-infected macaques (SHIVIG), with or without b12, in the 1-month-old rhesus macaques. The goal of these experiments was not to block infection but to understand the effects of neutralizing IgG in the presence of infection on pathogenesis and the development of *de novo* adaptive responses *in vivo*, as had been observed in the pathogenic SIV/macaque model (20). The rationale for the inclusion of b12 was to begin to address whether supplementation of maternal IgG with one or more human NMAb could be a valid approach to be used in the clinics to prevent mother-to-child transmission (MTCT) of HIV-1. SHIVIG was subcutaneously administered at a dose normalized for neutralization activity and based on neutralization (AID_{50}) titers in plasma of infected infants from previous work in pigtails (25). To study the potential benefit of augmenting SHIVIG with a CD4 binding site-directed neutralizing antibody, we combined b12 with SHIVIG at a ratio of 1:1,000 (wt/wt).

Passively transferred SHIVIG concentrations and neutralization activity against $SHIV_{SF162P3}$ were measured in plasma at the time of challenge (see Fig. S1A and B in the supplemental material). SHIVIG only (formulation B; see Table S3) blocked infection in five of six animals and four of six infants treated with SHIVIG plus b12 (Fig. 1C and D). These protection data clearly show the potency of the SHIVIG in blocking against oral challenge. In the protected macaques, we monitored the concentrations of SHIVIG and SHIVIG plus b12 by ELISA and used neutralization to predict an optimal time for rechallenge in order to test the effects of SHIVIG at a nonsterilizing dose. We rechallenged the five uninfected animals treated with SHIVIG only 3 weeks later, after the SHIVIG plasma concentration and plasma NAb titers had de-

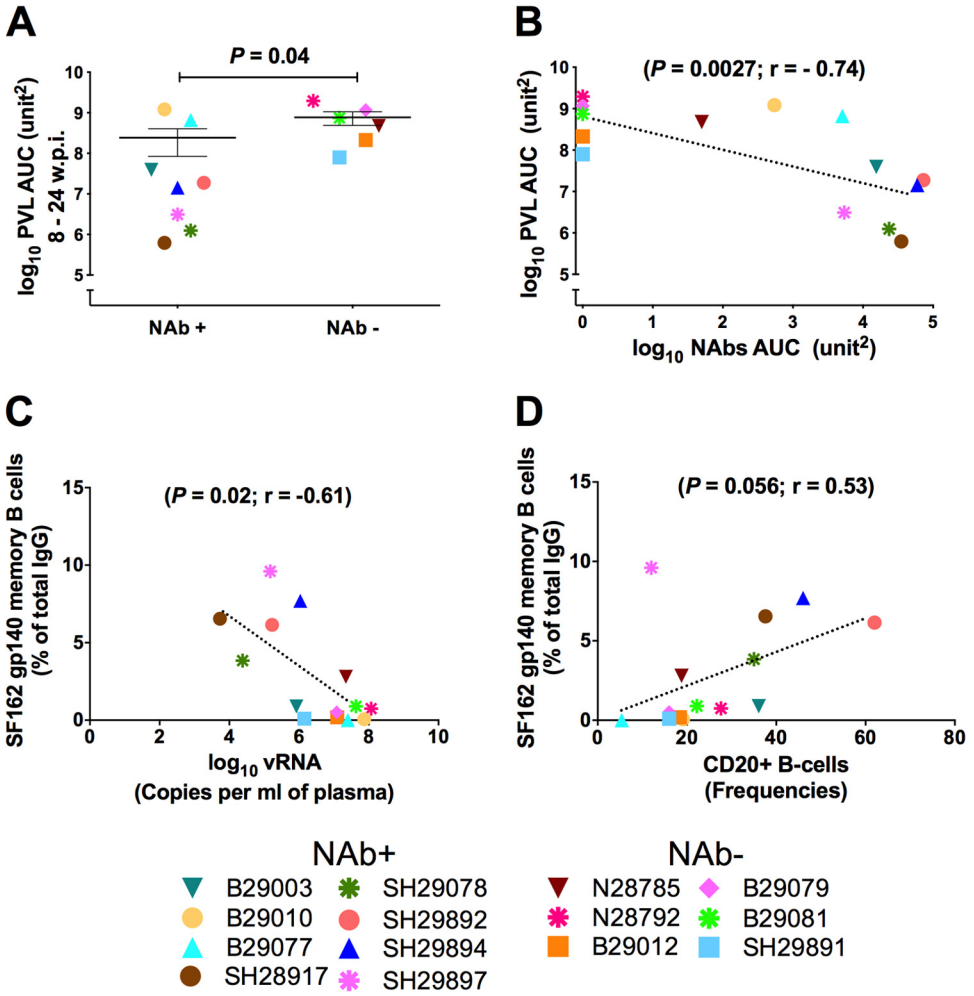

FIG 6 Correlations between plasma virus load and NAbs, antigen-specific (SF162 gp140) memory B cells, and B cell frequencies for macaques that developed NAbs and those that did not. (A) Plasma viral loads between weeks 8 and 24; (B) inverse correlation of PVL (weeks 8 to 24) *de novo* NAb development (weeks 6 to 24) during set-point viremia. Correlations of HIV-1_{SF162} gp140-specific memory B cells were determined by ELISPOT assay with plasma viral loads measured at the time of necropsy (C) and with total peripheral $CD20^+$ B cell frequencies, quantified by flow cytometry, at necropsy (D). NAb^+ and NAb^- animals are identified individually. Analysis includes only infected *Mamu-B*08*- and *Mamu-B*17*-negative animals ($n = 14$). Spearman correlation was used, and *r* and *P* values are given.

cayed to one-third of the concentration measured at the time of the first challenge, and four of these remaining SHIVIG-treated animals became infected (Fig. 1C; an arrow denotes the second challenge). SHIVIG-plus-b12-treated infants were not rechallenged, as b12 had decayed to the baseline.

Prechallenge transfer of SHIVIG modulates peak and chronic viremia. To determine the impact of SHIVIG on infection, we compared *Mamu-B*17*- and *Mamu-B*08*-negative infected infants that received SHIVIG (SHIVIG; $n = 6$) to those that were infused with normal IgG or normal IgG plus b12 (No-SHIVIG; $n = 8$) (Fig. 3). The plasma viral loads during acute infection of all *Mamu-B*08/17* allele-negative animals receiving normal IgG only or normal IgG plus b12 were not distinguishable. Peak viremia was significantly lower in SHIVIG than No-SHIVIG animals (1.3×10^7 and 7.1×10^7 copies/ml, respectively; $P = 0.02$) (Fig. 3C). Moreover, the total virus load, calculated as the AUC over the entire 24-week observation period, was also significantly lower in SHIVIG than No-SHIVIG animals ($P = 0.001$) (Fig. 3D). Plasma viral load was correlated with peripheral blood mononuclear cell-associated viral load for each infected animal ($P = 0.0004$; $r = 0.81$; $n = 14$) (Fig. 4A) and was significantly lower in SHIVIG than No-SHIVIG animals ($P = 0.009$) (Fig. 4B), indicating SHIVIG control of $SHIV_{SF162P3}$ viral dissemination as well as plasma viremia. The presence of less than sterilizing levels of SHIVIG at the time of challenge resulted in a reduction of both peak and total virus load in plasma and burden of integrated virus in PBMC, as previously observed with SIVIG (20).

SHIVIG promotes early and prolonged endogenous NAbs and ADCVI. To determine the impact of SHIVIG upon *de novo* antibody production, we measured Env-specific antibodies and NAbs against $SHIV_{SF162P3}$ (see Fig. S2 in the supplemental material). We differentiated endogenous from SHIVIG NAbs by examining the neutralization activity in the plasma of the four uninfected animals in the SHIVIG-plus-b12 group. By week six after passive infusion of the SHIVIG, we did not detect any neutralizing activity in the plasma samples from these animals (see Fig. S2, bottom right), indicating that in the absence of antigenic stimulation and endogenous NAb production, passively administered

TABLE 1 Pathology summary of $SHIV_{SF162P3}$-infected newborn rhesus macaques[d]

Group and animal ID[a]	NAb status[b]	Disease score[c]	Opportunistic infections and pathological diagnoses
Normal IgG plus b12			
B29081	NAb^-	3	Chronic active typhlocolitis; mild *Pneumocystis* pneumonia; diarrhea and dehydration
B29012	NAb^-	3	Chronic active typhlocolitis; cryptosporidial cholangiohepatitis, cholangitis and pancreatic duct inflammation; mild adenoviral nephritis; maculopapular rash ~2 wk postinoculation
B29077	NAb^+ wk 10	3	Cryptosporidial tracheitis, cholangiohepatitis, cholangitis, and pancreatic duct inflammation; flagellate enteritis; serositis and mesenteric lymphadenitis due to *Spironucleus*; severe adenoviral pancreatitis, nephritis, and cystitis; viral enteritis
B29079	NAb^-	2	SHIV giant cell pneumonia; *Pneumocystis* pneumonia; cryptosporidial tracheitis; serositis and mesenteric lymphadenitis due to *Spironucleus* species; choledochitis, cholecystitis, and pancreatic duct inflammation due to *Enterocytozoon bieneusi*; flagellate enteritis; adenoviral enteritis
B29010	NAb^+ wk 20	1	*Pneumocystis* pneumonia; adenoviral pancreatitis, cholecystitis, gastritis, and enteritis; mesenteric lymphadenitis due to *Spironucleus* species; diarrhea and leukocytosis
B29003	NAb^+ wk 8	1	None
Normal IgG only			
N28792	NAb^-	3	Chronic active typhlocolitis; cryptosporidial enteritis; cholangitis; adenoviral pancreatitis
N28785	NAb^-	3	Bacterial pneumonia, cytomegaloviral nephritis, vasculitis, and hepatitis; choledochitis, cholecystitis, and pancreatic duct inflammation due to *Enterocytozoon bieneusi*; flagellate ileocolitis, cryptosporidial gastroenteritis; enterocolitis and mesenteric lymphadenitis due to *Spironucleus* species; proliferative vasculitis
N28791*	NAb^+ wk 8	1	Choledochitis and cholecystitis due to *Enterocytozoon bieneusi*; chronic active typhlocolitis; flagellate colitis
N28779*	NAb^+ wk 12	1	None
N28776*	NAb^+ wk 10	0	None
N28778*	NAb^+ wk 10	0	Focal proliferative vasculitis; mild pancreatitis
SHIVIG			
SH29891	NAb^-	3	Choledochitis, cholecystitis, and pancreatic duct inflammation due to *Enterocytozoon bieneusi*; adenoviral pancreatitis, flagellate and amebic enterocolitis
SH29892	NAb^+ wk 6	1	Esophageal leukoplakia; mild enteritis with villous atrophy
SH29896**	NAb^+ wk 6	1	Intermittent diarrhea
SH29897	NAb^+ wk 6	0	Flagellate gastritis; chronic active colitis
SH29894	NAb^+ wk 6	0	Mild choledochitis, cholecystitis, and pancreatic duct inflammation due to *Enterocytozoon bieneusi*; flagellate gastritis
SHIVIG plus b12			
SH28917	NAb^+ wk 6	0	None
SH29078	NAb^+ wk 6	0	None

[a] *, *Mamu* B*008:01 positive; **, *Mamu* B*017:01 positive.
[b] NAb^+ status includes the timing of development of *de novo* neutralizing antibodies. NAb^- status indicates no *de novo* neutralizing antibody development.
[c] Disease scores are the following: 3, clinically ill prompting early termination; 2, clinically ill; 1, mild illness; 0, clinically healthy.
[d] Uninfected animals are not included. All remained clinically healthy throughout the study period.

NAb (SHIVIG) is cleared from the plasma by that time. At week six, when passively transferred NAbs had decayed, the mean NAb titers were significantly higher in SHIVIG than No-SHIVIG macaques ($P = 0.029$) (Fig. 5A) and were analyzed for individual animals in these two groups ($P = 0.011$) (Fig. 5B). Five No-SHIVIG macaques failed to develop NAbs, indicating more rapid development of *de novo* NAb responses in SHIVIG animals. At necropsy, NAbs remained significantly higher in SHIVIG than in No-SHIVIG animals ($P = 0.025$) (Fig. 5C). ADCVI activity was significantly greater in SHIVIG macaques at week 6 ($P = 0.01$) (Fig. 5D). Altogether, and as we have seen previously (25), the data indicate the passive administration of SHIVIG potentiated early and potent *de novo* NAb and ADCVI responses in macaque infants with naive immune systems.

When we analyzed the impact of the *de novo* production of NAbs on set-point viremia, we found that irrespective of the treatment, infected animals that produced endogenous NAb responses (NAb^+) had significantly lower set-point viremia than NAb^- animals ($P = 0.04$; $n = 14$) (Fig. 6A). The development of *de novo* NAbs was inversely correlated with plasma viral load ($P = 0.0027$; $r = -0.74$) (Fig. 6B). In NAb^+ animals, Env-specific memory B cells inversely correlated with plasma viral load ($P = 0.02$; $r = -0.61$) (Fig. 6C) and positively correlated with maintenance of peripheral B cell frequencies at the time of necropsy ($P = 0.056$; $r = 0.53$) (Fig. 6D), supporting a role for B cells in viremia control.

Survival is associated with NAb development and both T and B cell preservation. The 1-month-old rhesus macaques in this study with uncontrolled viremia progressed rapidly to clinical dis-

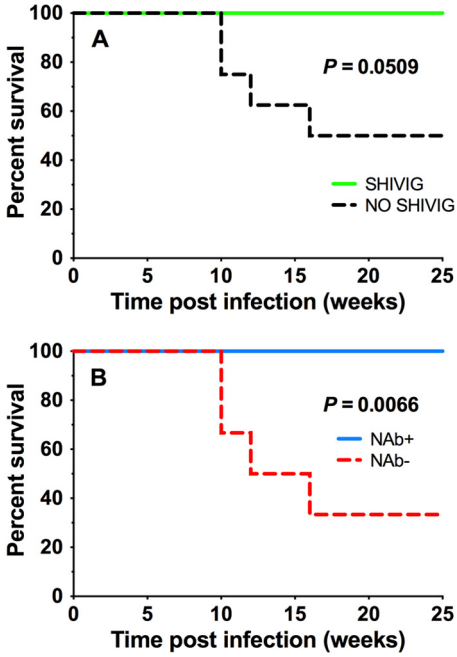

FIG 7 Kaplan-Meier survival curves for $SHIV_{SF162P3}$-infected infant macaques. (A) Four NAb^-/No-SHIVIG animals were euthanized by week 16 for humane reasons due to severe disease progression (Table 1). Analysis includes only infected *Mamu-B*008:01*- and *Mamu-B*017:01*-negative animals ($n = 14$). (B) NAb^+ and NAb^- animals are identified in Table 1. Log-rank (Mantel-Cox) test was used to compare survival curves. *P* values are indicated.

ease, and several required euthanasia (Table 1). This table also includes the *Mamu-B*08*/*17* allele-positive animals, all of which had low disease scores of 0 or 1. In contrast, all of those with disease scores of 3 were in the normal IgG groups. All SHIVIG-treated macaques survived, while four of the eight in the No-SHIVIG group were euthanized ($P = 0.0509$) (Fig. 7A). Upon analysis, we found that survival of NAb^+ animals was significantly increased compared to that of NAb^- animals ($P = 0.0066$) (Fig. 7B). At necropsy, all six NAb^- animals presented severe clinical symptoms with opportunistic infections, including profound weight loss and evidence of prolonged diarrhea, as well as abnormalities in systemic lymph nodes, spleen, and thymus, associated with profound lymphocyte depletion. In stark contrast, 12/13 NAb^+ animals showed no symptoms of advanced disease (Table 1).

Total peripheral $CD4^+$ and $CD8^+$ T cell counts remained similar between NAb^+ and NAb^- groups over the entire 24 weeks of study. At necropsy, a trend toward lower $CD4^+$ T cells was seen in NAb^- compared to NAb^+ and uninfected animals, but the difference did not reach statistical significance, and there were no significant differences in $CD8^+$ T cells (see Fig. S3A and B in the supplemental material). However, despite maintaining $CD4^+$ T cell counts in a range from 474 to 1,880 $CD4^+$ T cells/μl of blood, four of six NAb^- animals developed severe and debilitating symptoms of disease and were euthanized by 16 weeks after exposure (Table 1 and Fig. 7B). These observations suggest that a deficit in NAbs is associated with rapid disease progression regardless of $CD4^+$ T cell counts, as we previously observed in SIV infection (20). T cells obtained by BAL fluid taken at necropsy were analyzed for intracellular cytokine expression, and all responses were very low, with no significant difference between groups (data not shown).

MHC genotype reduces pathogenesis and shields against B cell dysregulation. Finally, to determine whether B cells were similarly preserved in the No-SHIVIG *Mamu-B*08*/*B*17*-positive macaques, we compared the NAbs and B cell frequencies in these macaques to those in the SHIVIG group. During acute infection (from 0 to 8 weeks p.i.), viremia was extremely high and significantly higher in No-SHIVIG animals without either of the protective alleles than in No-SHIVIG animals that carried the alleles ($P < 0.05$) or SHIVIG animals that were *Mamu-B*08*/*B*17* negative ($P < 0.01$) (Fig. 8A). We also found that without the benefit of SHIVIG, animals without *Mamu* allele *B*08* or *B*17* had significantly fewer peripheral $CD20^+$ B cells than the other two groups during acute infection (Fig. 8B). Moreover, acute viremia was inversely correlated with the level of the endogenous NAb response ($P = 0.005$; $r = -0.61$) (Fig. 8C). Altogether, these data suggest that an early B cell dysregulation was provoked by the extremely high acute viremia in the No-SHIVIG/*Mamu-B*08*/*B*17*-negative animals, resulting in failure to develop persistent NAbs in five of eight of these animals (Fig. 8D; note that N28785 was weakly positive at a single time point, week 12; also see Fig. S2B in the supplemental material).

DISCUSSION

This study, as well as our prior work in pigtail macaques (24, 25), demonstrates that high, acute, and persistent plasma viremia is routinely observed in untreated 1-month-old macaques challenged with $SHIV_{SF162P3}$, and it differs from that observed in older rhesus macaques challenged with the same virus (22). A major difference between the pigtail and rhesus macaques is the pathogenic consequences of infection with this strain of SHIV. In stark contrast to the pigtail study, four of six rhesus macaques that failed to generate *de novo* NAbs progressed to AIDS and death. One of the unusual aspects of rapid progression in SIV infection of macaques is that antibody production is low or undetectable (20, 43), often limited to IgM with little or no detection of IgG. Pathogenesis is more pronounced in very young macaques and has been observed following vaccination with live attenuated SIV (44). Thus, in many aspects, the infection of 1-month-old rhesus macaques with $SHIV_{SF162P3}$ has the hallmarks of SIVmac239 infection in juveniles. Untreated or unvaccinated animals experience high levels of plasma and cell-associated viremia, failure to develop significant NAbs within the first 6 months of infection, and loss of B cells (10).

In this study, passive administration of 100 to 200 mg/kg of neutralizing SHIVIG before oral challenge with $SHIV_{SF162P3}$ protected 9 of 12 1-month-old rhesus macaques from infection. When rechallenged after SHIVIG levels waned to a dose equivalent to ~30 mg/kg, one of five infants was protected. Infected infants that received SHIVIG developed an endogenous NAb response more rapidly, had reduced set-point plasma and cell-associated viremia, and showed ameliorated disease pathogenesis, leading to 100% survival of NAb^+ animals. In this experimental system, NAbs were matched to the challenge virus. Importantly, the effects of SHIVIG were obtained using IgG purified from macaques that had only autologous neutralizing activity, indicating that this response is sufficiently potent in the setting of a matched virus challenge. We were unable to determine whether adding b12 to the mixture of polyclonal IgG (SHIVIG) at the small dose tested

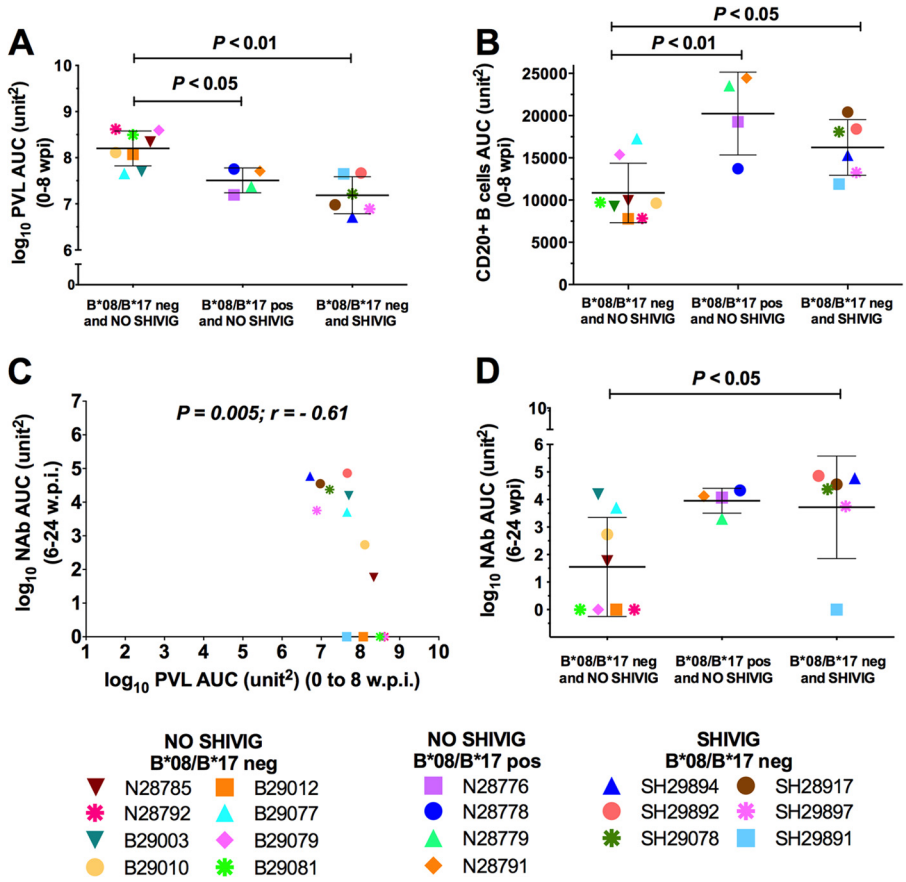

FIG 8 MHC-I alleles promote endogenous NAb responses. Comparison during acute infection (weeks 0 to 8) of No-SHIVIG animals (*Mamu-B*08* and *Mamu-B*17* positive and negative) and SHIVIG animals (*Mamu-B*08* and *Mamu-B*17* negative) for PVL (A) and peripheral CD20$^+$ B cells (B). (C) Inverse correlation of acute viremia and endogenous *de novo* NAb response (weeks 6 to 24) and (D) comparison of endogenous NAb responses between the three groups. The *P* values and the correlation coefficient (*r*) are stated. Bonferroni and Tukey-Kramer adjustment for multiple-error correction was used to determine the significance of multiple-group (3 or more) comparisons.

further improved its effectiveness *in vivo*. Further studies in this model with monoclonal and polyclonal antibodies are warranted to test these concepts in the setting of nonhomologous virus challenge. Our prior study of 1-month-old *M. nemestrina* animals showed that matching the SHIVIG to the challenge virus was critical to obtaining benefit (25). Thus, it is likely that if passive antibody-based therapy were to be effective, combinations or cocktails of broadly neutralizing as well as potent MAbs would be necessary. Nonetheless, in this setting, we documented the beneficial effects of polyclonal neutralizing Ig at the onset of severe and persistent SHIV viremia, as previously described for SIV infection (26, 27) and for one strain of SHIV infection in *Mamu-A*01*-negative macaques (42).

Class I alleles *Mamu-B*08* and *Mamu-B*17* are known to restrict responses to SIV_{mac239} Vif and Nef, which are present in $SHIV_{SF162P3}$. Indeed, *Mamu-B*08*- and *Mamu-B*17*-positive animals targeted Vif and Nef with CD8$^+$ T cell responses restricted by these two MHC-I molecules. Intriguingly, *Mamu-B*08*- and *Mamu-B*17*-positive animals still contained $SHIV_{SF162P3}$ replication despite lacking *Mamu-B*08*- and *Mamu-B*17*-bound epitopes found within SIVmac239 Env. Further, we saw similarities in the reduced pathogenesis between SHIVIG/*Mamu-B*008:01*- and *Mamu-B*017:01*-negative animals and the No-SHIVIG/*Mamu-B*08*- and *Mamu-B*17*-positive infected animals at 1 month of age. This is an interesting parallel that suggests that reduction of viremia by different mechanisms can lead to similar disease outcomes. Alternatively, it is possible that the passive IgG has directly limited viremia, leading to early viral control by T cell-based mechanisms. However, we did not measure strong T cell responses during the acute phase in PBMC, suggesting that NAbs present during primary viremia can limit viral spread and pathogenesis even in the absence of protective MHC-I alleles, leading to strong adaptive responses and a more favorable outcome of infection. Future studies in nonhuman primate models are warranted to understand the mechanisms by which NAbs are contributing to enhanced B cell immunity and better disease control.

The SHIVIG preparations used in this study were pools of IgG produced in response to infection during the first few months of infection; thus, they were capable of neutralizing only the homologous virus. Nevertheless, SHIVIG had profound effects upon the ability of the host to control the matched challenge virus. Most Env-based vaccine studies performed to date generate NAbs with limited breadth, and increasing the effectiveness of these NAbs in blocking heterologous strains remains a key objective. Testing the potential protective and immunomodulatory effectiveness of antibodies elicited by different vaccine approaches will be a rate-limiting step that could benefit from direct testing in this model.

These studies also provide further impetus for pursuing preexposure prophylaxis with cocktails of human NMAbs with potent, broad activity to be used along with antiretroviral therapy (ART). Such experiments can be modeled in the nonhuman primate model we describe here. If these experiments yield the predicted positive outcome, they may also provide a rationale for moving NMAb cocktails to the clinic to complement maternal ART or preexposure ART prophylaxis (PrEP) to enhance viral control or to prevent infection.

ACKNOWLEDGMENTS

We are grateful for the expert animal care and technical assistance provided by Shannon Planer, Merete Ohme, Megan O'Brien, and Adriane Maier. We thank Kim Wahl for assistance with necropsies and histology, Leo Stamatatos for providing envelope gp140 for ELISAs, and Steve Dewhurst and the University of Rochester D-CFAR Recombinant Protein Core for providing gp140 for the ELISPOT assay.

This work was supported by grants from the Elizabeth Glaser Pediatric AIDS Foundation to N.L.H., U.S. National Institutes of Health grants P51 OD011092 (ONPRC), U42 RR016025 (ONPRC), and R01 HD38653 to N.L.H., U19 AI067854 to J.K., and R01 AI55332 to D.R.B.

J.P.J., I.M., J.K., J.B.S., D.R.B., D.N.F., A.J.H., and N.L.H. wrote the manuscript. J.P.J., Z.B., J.K., J.S.R., E.J.L., D.C.M., G.L., W.F.S., B.G., F.E., B.Z., A.L., M.D., A.D.L., L.M.A.C., and M.K.A. performed experiments. D.R.B. contributed reagents. J.P.J., B.P., I.M., D.C.M., J.K., A.L., M.K.A., J.B.S., M.D., A.D.L., L.M.A.C., N.L.H., A.J.H., and D.N.F. analyzed the data.

REFERENCES

1. **Gray ES, Madiga MC, Hermanus T, Moore PL, Wibmer CK, Tumba NL, Werner L, Mlisana K, Sibeko S, Williamson C, Abdool Karim SS, Morris L.** 2011. The neutralization breadth of HIV-1 develops incrementally over four years and is associated with CD4+ T cell decline and high viral load during acute infection. J. Virol. **85:**4828–4840.
2. **Richman DD, Wrin T, Little SJ, Petropoulos CJ.** 2003. Rapid evolution of the neutralizing antibody response to HIV type 1 infection. Proc. Natl. Acad. Sci. U. S. A. **100:**4144–4149.
3. **Sather DN, Armann J, Ching LK, Mavrantoni A, Sellhorn G, Caldwell Z, Yu X, Wood B, Self S, Kalams S, Stamatatos L.** 2009. Factors associated with the development of cross-reactive neutralizing antibodies during human immunodeficiency virus type 1 infection. J. Virol. **83:**757–769.
4. **Wei X, Decker JM, Wang S, Hui H, Kappes JC, Wu X, Salazar-Gonzalez JF, Salazar MG, Kilby JM, Saag MS, Komarova NL, Nowak MA, Hahn BH, Kwong PD, Shaw GM.** 2003. Antibody neutralization and escape by HIV-1. Nature **422:**307–312.
5. **Burton DR, Pyati J, Koduri R, Sharp SJ, Thornton GB, Parren PWHI, Sawyer LSW, Hendry RM, Dunlop N, Nara PL, Lamacchia M, Garratty E, Stiehm ER, Bryson YJ, Cao Y, Moore JP, Ho DD, Barbas CF, III.** 1994. Efficient neutralization of primary isolates of HIV-1 by a recombinant human monoclonal antibody. Science **266:**1024–1027.
6. **Huang J, Ofek G, Laub L, Louder MK, Doria-Rose NA, Longo NS, Imamichi H, Bailer RT, Chakrabarti B, Sharma SK, Alam SM, Wang T, Yang Y, Zhang B, Migueles SA, Wyatt R, Haynes BF, Kwong PD, Mascola JR, Connors M.** 2012. Broad and potent neutralization of HIV-1 by a gp41-specific human antibody. Nature **491:**406–412.
7. **Walker LM, Phogat SK, Chan-Hui PY, Wagner D, Phung P, Goss JL, Wrin T, Simek MD, Fling S, Mitcham JL, Lehrman JK, Priddy FH, Olsen OA, Frey SM, Hammond PW, Kaminsky S, Zamb T, Moyle M, Koff WC, Poignard P, Burton DR.** 2009. Broad and potent neutralizing antibodies from an African donor reveal a new HIV-1 vaccine target. Science **326:**285–289.
8. **Wu X, Yang ZY, Li Y, Hogerkorp CM, Schief WR, Seaman MS, Zhou T, Schmidt SD, Wu L, Xu L, Longo NS, McKee K, O'Dell S, Louder MK, Wycuff DL, Feng Y, Nason M, Doria-Rose N, Connors M, Kwong PD, Roederer M, Wyatt RT, Nabel GJ, Mascola JR.** 2010. Rational design of envelope identifies broadly neutralizing human monoclonal antibodies to HIV-1. Science **329:**856–861.
9. **Moir S, Ho J, Malaspina A, Wang W, DiPoto AC, O'Shea MA, Roby G, Kottilil S, Arthos J, Proschan MA, Chun TW, Fauci AS.** 2008. Evidence for HIV-associated B cell exhaustion in a dysfunctional memory B cell compartment in HIV-infected viremic individuals. J. Exp. Med. **205:**1797–1805.
10. **Kuhrt D, Faith SA, Leone A, Rohankedkar M, Sodora DL, Picker LJ, Cole KS.** 2010. Evidence of early B-cell dysregulation in simian immunodeficiency virus infection: rapid depletion of naive and memory B-cell subsets with delayed reconstitution of the naive B-cell population. J. Virol. **84:**2466–2476.
11. **Peruchon S, Chaoul N, Burelout C, Delache B, Brochard P, Laurent P, Cognasse F, Prevot S, Garraud O, Le Grand R, Richard Y.** 2009. Tissue-specific B-cell dysfunction and generalized memory B-cell loss during acute SIV infection. PLoS One **4:**e5966. doi:10.1371/journal.pone.0005966.
12. **Levesque MC, Moody MA, Hwang KK, Marshall DJ, Whitesides JF, Amos JD, Gurley TC, Allgood S, Haynes BB, Vandergrift NA, Plonk S, Parker DC, Cohen MS, Tomaras GD, Goepfert PA, Shaw GM, Schmitz JE, Eron JJ, Shaheen NJ, Hicks CB, Liao HX, Markowitz M, Kelsoe G, Margolis DM, Haynes BF.** 2009. Polyclonal B cell differentiation and loss of gastrointestinal tract germinal centers in the earliest stages of HIV-1 infection. PLoS Med. **6:**e1000107. doi:10.1371/journal.pmed.1000107.
13. **Boliar S, Murphy MK, Tran TC, Carnathan DG, Armstrong WS, Silvestri G, Derdeyn CA.** 2012. B-lymphocyte dysfunction in chronic HIV-1 infection does not prevent cross-clade neutralization breadth. J. Virol. **86:**8031–8040.
14. **Hart M, Steel A, Clark SA, Moyle G, Nelson M, Henderson DC, Wilson R, Gotch F, Gazzard B, Kelleher P.** 2007. Loss of discrete memory B cell subsets is associated with impaired immunization responses in HIV-1 infection and may be a risk factor for invasive pneumococcal disease. J. Immunol. **178:**8212–8220.
15. **Baba TW, Liska V, Hofmann-Lehmann R, Vlasak J, Xu W, Ayehunie S, Cavacini LA, Posner MR, Katinger H, Stiegler G, Bernacky BJ, Rizvi TA, Schmidt R, Hill LR, Keeling ME, Lu Y, Wright JE, Chou TC, Ruprecht RM.** 2000. Human neutralizing monoclonal antibodies of the IgG1 subtype protect against mucosal simian-human immunodeficiency virus infection. Nat. Med. **6:**200–206.
16. **Mascola JR, Stiegler G, VanCott TC, Katinger H, Carpenter CB, Hanson CE, Beary H, Hayes D, Frankel SS, Birx DL, Lewis MG.** 2000. Protection of macaques against vaginal transmission of a pathogenic HIV-1/SIV chimeric virus by passive infusion of neutralizing antibodies. Nat. Med. **6:**207–210.
17. **Parren PW, Marx PA, Hessell AJ, Luckay A, Harouse J, Cheng-Mayer C, Moore JP, Burton DR.** 2001. Antibody protects macaques against vaginal challenge with a pathogenic R5 simian/human immunodeficiency virus at serum levels giving complete neutralization in vitro. J. Virol. **75:**8340–8347.
18. **Shibata R, Igarashi T, Haigwood N, Buckler-White A, Ogert R, Ross W, Willey R, Cho MW, Martin MA.** 1999. Neutralizing antibody directed against the HIV-1 envelope glycoprotein can completely block HIV-1/SIV chimeric virus infections of macaque monkeys. Nat. Med. **5:**204–210.
19. **Hessell AJ, Poignard P, Hunter M, Hangartner L, Tehrani DM, Bleeker WK, Parren PW, Marx PA, Burton DR.** 2009. Effective, low-titer antibody protection against low-dose repeated mucosal SHIV challenge in macaques. Nat. Med. **15:**951–954.
20. **Haigwood NL, Montefiori DC, Sutton WF, McClure J, Watson AJ, Voss G, Hirsch VM, Richardson BA, Letvin NL, Hu SL, Johnson PR.** 2004. Passive immunotherapy in simian immunodeficiency virus-infected macaques accelerates the development of neutralizing antibodies. J. Virol. **78:**5983–5995.
21. **Yamamoto T, Iwamoto N, Yamamoto H, Tsukamoto T, Kuwano T, Takeda A, Kawada M, Tsunetsugu-Yokota Y, Matano T.** 2009. Polyfunctional CD4+ T-cell induction in neutralizing antibody-triggered control of simian immunodeficiency virus infection. J. Virol. **83:**5514–5524.
22. **Harouse JM, Gettie A, Eshetu T, Tan RC, Bohm R, Blanchard J, Baskin G, Cheng-Mayer C.** 2001. Mucosal transmission and induction of simian AIDS by CCR5-specific simian/human immunodeficiency virus SHIV(SF162P3). J. Virol. **75:**1990–1995.
23. **Polacino P, Larsen K, Galmin L, Suschak J, Kraft Z, Stamatatos L, Anderson D, Barnett SW, Pal R, Bost K, Bandivdekar AH, Miller CJ, Hu SL.** 2008. Differential pathogenicity of SHIV infection in pig-tailed and rhesus macaques. J. Med. Primatol. **37**(Suppl. 2):13–23.

24. **Jayaraman P, Zhu T, Misher L, Mohan D, Kuller L, Polacino P, Richardson BA, Bielefeldt-Ohmann H, Anderson D, Hu SL, Haigwood NL.** 2007. Evidence for persistent, occult infection in neonatal macaques following perinatal transmission of simian-human immunodeficiency virus SF162P3. J. Virol. **81:**822–834.
25. **Ng CT, Jaworski JP, Jayaraman P, Sutton WF, Delio P, Kuller L, Anderson D, Landucci G, Richardson BA, Burton DR, Forthal DN, Haigwood NL.** 2010. Passive neutralizing antibody controls SHIV viremia and enhances B cell responses in infant macaques. Nat. Med. **16:**1117–1119.
26. **Loffredo JT, Maxwell J, Qi Y, Glidden CE, Borchardt GJ, Soma T, Bean AT, Beal DR, Wilson NA, Rehrauer WM, Lifson JD, Carrington M, Watkins DI.** 2007. Mamu-B*08-positive macaques control simian immunodeficiency virus replication. J. Virol. **81:**8827–8832.
27. **Yant LJ, Friedrich TC, Johnson RC, May GE, Maness NJ, Enz AM, Lifson JD, O'Connor DH, Carrington M, Watkins DI.** 2006. The high-frequency major histocompatibility complex class I allele Mamu-*B*17* is associated with control of simian immunodeficiency virus SIVmac239 replication. J. Virol. **80:**5074–5077.
28. **Tan RC, Harouse JM, Gettie A, Cheng-Mayer C.** 1999. In vivo adaptation of SHIV(SF162): chimeric virus expressing a NSI, CCR5-specific envelope protein. J. Med. Primatol. **28:**164–168.
29. **Long EM, Rainwater SM, Lavreys L, Mandaliya K, Overbaugh J.** 2002. HIV type 1 variants transmitted to women in Kenya require the CCR5 coreceptor for entry, regardless of the genetic complexity of the infecting virus. AIDS Res. Hum. Retrovir. **18:**567–576.
30. **Li M, Gao F, Mascola JR, Stamatatos L, Polonis VR, Koutsoukos M, Voss G, Goepfert P, Gilbert P, Greene KM, Bilska M, Kothe DL, Salazar-Gonzalez JF, Wei X, Decker JM, Hahn BH, Montefiori DC.** 2005. Human immunodeficiency virus type 1 env clones from acute and early subtype B infections for standardized assessments of vaccine-elicited neutralizing antibodies. J. Virol. **79:**10108–10125.
31. **Malherbe DC, Doria-Rose NA, Misher L, Beckett T, Puryear WB, Schuman JT, Kraft Z, O'Malley J, Mori M, Srivastava I, Barnett S, Stamatatos L, Haigwood NL.** 2011. Sequential immunization with a subtype B HIV-1 envelope quasispecies partially mimics the in vivo development of neutralizing antibodies. J. Virol. **85:**5262–5274.
32. **Forthal DN, Gilbert PB, Landucci G, Phan T.** 2007. Recombinant gp120 vaccine-induced antibodies inhibit clinical strains of HIV-1 in the presence of Fc receptor-bearing effector cells and correlate inversely with HIV infection rate. J. Immunol. **178:**6596–6603.
33. **Kaizu M, Borchardt GJ, Glidden CE, Fisk DL, Loffredo JT, Watkins DI, Rehrauer WM.** 2007. Molecular typing of major histocompatibility complex class I alleles in the Indian rhesus macaque which restrict SIV CD8+ T cell epitopes. Immunogenetics **59:**693–703.
34. **Reynolds MR, Weiler AM, Weisgrau KL, Piaskowski SM, Furlott JR, Weinfurter JT, Kaizu M, Soma T, Leon EJ, MacNair C, Leaman DP, Zwick MB, Gostick E, Musani SK, Price DA, Friedrich TC, Rakasz EG, Wilson NA, McDermott AB, Boyle R, Allison DB, Burton DR, Koff WC, Watkins DI.** 2008. Macaques vaccinated with live-attenuated SIV control replication of heterologous virus. J. Exp. Med. **205:**2537–2550.
35. **Haberthur K, Engelmann F, Park B, Barron A, Legasse A, Dewane J, Fischer M, Kerns A, Brown M, Messaoudi I.** 2011. CD4 T cell immunity is critical for the control of simian varicella virus infection in a nonhuman primate model of VZV infection. PLoS Pathog. **7:**e1002367. doi:10.1371/journal.ppat.1002367.
36. **Salazar-Gonzalez JF, Bailes E, Pham KT, Salazar MG, Guffey MB, Keele BF, Derdeyn CA, Farmer P, Hunter E, Allen S, Manigart O, Mulenga J, Anderson JA, Swanstrom R, Haynes BF, Athreya GS, Korber BT, Sharp PM, Shaw GM, Hahn BH.** 2008. Deciphering human immunodeficiency virus type 1 transmission and early envelope diversification by single-genome amplification and sequencing. J. Virol. **82:**3952–3970.
37. **Pantophlet R, Ollmann Saphire E, Poignard P, Parren PW, Wilson IA, Burton DR.** 2003. Fine mapping of the interaction of neutralizing and nonneutralizing monoclonal antibodies with the CD4 binding site of human immunodeficiency virus type 1 gp120. J. Virol. **77:**642–658.
38. **Poignard P, Sabbe R, Picchio GR, Wang M, Gulizia RJ, Katinger H, Parren PW, Mosier DE, Burton DR.** 1999. Neutralizing antibodies have limited effects on the control of established HIV-1 infection in vivo. Immunity **10:**431–438.
39. **Sundling C, Forsell MN, O'Dell S, Feng Y, Chakrabarti B, Rao SS, Lore K, Mascola JR, Wyatt RT, Douagi I, Karlsson Hedestam GB.** 2010. Soluble HIV-1 Env trimers in adjuvant elicit potent and diverse functional B cell responses in primates. J. Exp. Med. **207:**2003–2017.
40. **Mattiacio J, Walter S, Brewer M, Domm W, Friedman AE, Dewhurst S.** 2011. Dense display of HIV-1 envelope spikes on the lambda phage scaffold does not result in the generation of improved antibody responses to HIV-1 Env. Vaccine **29:**2637–2647.
41. **Hessell AJ, Rakasz EG, Poignard P, Hangartner L, Landucci G, Forthal DN, Koff WC, Watkins DI, Burton DR.** 2009. Broadly neutralizing human anti-HIV antibody 2G12 is effective in protection against mucosal SHIV challenge even at low serum neutralizing titers. PLoS Pathog. **5:**e1000433. doi:10.1371/journal.ppat.1000433.
42. **Mao H, Lafont BA, Igarashi T, Nishimura Y, Brown C, Hirsch V, Buckler-White A, Sadjadpour R, Martin MA.** 2005. CD8+ and CD20+ lymphocytes cooperate to control acute simian immunodeficiency virus/human immunodeficiency virus chimeric virus infections in rhesus monkeys: modulation by major histocompatibility complex genotype. J. Virol. **79:**14887–14898.
43. **Hirsch VM, Santra S, Goldstein S, Plishka R, Buckler-White A, Seth A, Ourmanov I, Brown CR, Engle R, Montefiori D, Glowczwskie J, Kunstman K, Wolinsky S, Letvin NL.** 2004. Immune failure in the absence of profound CD4+ T-lymphocyte depletion in simian immunodeficiency virus-infected rapid progressor macaques. J. Virol. **78:**275–284.
44. **Baba TW, Jeong YS, Penninck D, Bronson R, Greene MF, Ruprecht RM.** 1995. Pathogenicity of live, attenuated SIV after mucosal infection of neonatal macaques. Science **267:**1820–1825.